The Reactions $Al(^2P) + H_2 \rightarrow AlH_2(1^2A', 2^2A') \rightarrow AlH_2(X^2A_1)$ or $AlH(X^1\Sigma^+) + H$: Unusual Conical Intersections and Possible Nonadiabatic Recrossing

Galina Chaban[†] and Mark S. Gordon*[,†]

Department of Chemistry, Iowa State University, Ames, Iowa

David R. Yarkony*[,‡]

Department of Chemistry, The Johns Hopkins University, Baltimore, Maryland 21218

Received: May 15, 1997; In Final Form: July 8, 1997[⊗]

The energies and derivative couplings are computed in the vicinity of the $1^2A'-2^2A'$ seam of conical intersections for AlH_2. It is shown that the reaction path for the decomposition of excited vibrational levels of $AlH_2(X^2A_1)$ to $Al + H_2$ passes quite close to the minimum energy crossing point (MECP), the minimum energy point on the seam of conical intersections. Near the MECP the seam of conical intersections exhibits an unusual trifurcation with a C_{2v} portion dividing into a branch that preserves C_{2v} symmetry and two symmetry equivalent branches that have only C_s symmetry.

I. Introduction

Characterization of the transition state for a chemical reaction is frequently key to understanding the reaction mechanism and determining the reaction rate. However, when the transition state is located in the vicinity of a conical intersection, the reaction rate may be affected by a phenomenon referred to as nonadiabatic recrossing,[1,2] in which branching to an upper, nonreactive, surface reduces the observed reaction rate on the ground-state potential energy surface. In this situation it is essential to characterize the relevant conical intersections and determine the interstate derivative couplings, $f_\tau^{JI}(\mathbf{R}) = \langle\Psi_J(\mathbf{r};\mathbf{R})|(\partial/\partial\tau)\Psi_I(\mathbf{r};\mathbf{R})\rangle_r$, that are responsible for the nonadiabatic effects. Here τ is one of the nuclear coordinates $\mathbf{R}$, and $\Psi_I(\mathbf{r};\mathbf{R})$ is the adiabatic electronic state with energy $E_I(\mathbf{R})$.

Nonadiabatic recrossing may be important in the reactions of ground-state $Al(^2P)$ with molecular hydrogen.

$$Al(^2P) + H_2 \rightarrow AlH_2(1^2A_1, 1^2B_2) \rightarrow AlH_2(X^2A_1) \quad (1a)$$

$$\rightarrow AlH(X^1\Sigma^+) + H \quad (1b)$$

These reactions are of considerable practical importance, being relevant to the use of Al-doped cryogenic hydrogen as an energetic material. The formation of the dihydride $AlH_2(X^2A_1)$, channel 1a, could limit the stability of the van der Waals complex $Al-H_2$ that constitutes the energetic material, while channel 1b may be involved in the combustion of the energetic material. Channel 1a, dihydride formation, is exoergic by ∼17 kcal/mol (ref 3), while the chemical reaction, channel 1b, is endoergic.[4] The 1^2A_1 potential energy surface has a high barrier, ∼76 kcal/mol, to the formation of the X^2A_1 dihydride.[3] Low-energy pathways to the dihydride involve the $^2B_2$ potential energy surface. In C_{2v} symmetry, pathways originating on the $^2B_2$ potential energy surface access the dihydride via a symmetry-allowed $^2B_2-^2A_1$ conical intersection. For these constrained pathways, the minimum energy crossing point (MECP), the minimum energy point on the $^2B_2-^2A_1$ conical intersection seam, represents the "transition state" for the reaction. However as discussed in section II a conical intersection point cannot be the true transition state, so that the true reaction path must involve C_s structures, avoiding points of conical intersection. For C_s structures the $^2A_1$ and $^2B_2$ states become the $1^2A'$ and $2^2A'$ states. Preliminary calculations suggest that at the transition state deviations from C_{2v} symmetry are small.[3] Thus nonadiabatic recrossing may affect the rate of dihydride formation or the reverse reaction, the decay of excited vibrational levels, resonances, of the dihydride, $AlH_2(X^2A_1, v^*)$.

This work considers the mechanism of reaction 1, providing an analysis of the region of the $1^2A'-2^2A'$ seam of conical intersection. This analysis will guide the construction of the potential energy surfaces and surfaces of derivative couplings for this reaction, which will be the subject of a future publication. It will emerge that in the vicinity of the MECP the apparently straightforward symmetry-allowed seam of conical intersection becomes unexpectedly difficult to characterize. This difficulty is found to reflect the existence of a trifurcation of the seam of intersection, equivalently, the intersection of two distinct seams of conical intersection. This unusual topology will result in complicated nonadiabatic nuclear dynamics.

Section II recapitulates the techniques, described in detail previously,[5] used to characterize this seam of conical intersection. Also described in that section is the electronic structure treatment of AlH_2. Section III presents the results of the calculations and the implications for reaction 1. Section IV summarizes and discusses directions for subsequent investigations.

II. Theoretical Approach

The electronic structure calculations employ multiconfigurational self-consistent-field (MCSCF)[6] configuration interaction (CI)[7] wave functions. In the MCSCF/CI approach the adiabatic electronic state, $\Psi_I(\mathbf{r};\mathbf{R})$, is expanded in a configuration state function (CSF)[7] basis:

$$\Psi_I(\mathbf{r};\mathbf{R}) = \sum_{\alpha=1}^{N^{CSF}} c_\alpha^I(\mathbf{R})\, \psi_\alpha(\mathbf{r};\mathbf{R}) \quad (2)$$

[†] Supported by AFOSR Grant F49620-95-1-0077.
[‡] Supported by AFOSR Grant F49620-96-1-0017.
[⊗] Abstract published in *Advance ACS Abstracts,* September 15, 1997.

S1089-5639(97)01612-5 CCC: $14.00

so that the $\mathbf{c}^I(\mathbf{R})$ satisfy

$$[\boldsymbol{H}(\mathbf{R}) - E_I(\mathbf{R})]\mathbf{c}^I(\mathbf{R}) = \mathbf{0} \tag{3}$$

where the molecular orbitals used to build the $\psi_\alpha(\mathbf{r};\mathbf{R})$ are obtained from a state-averaged MCSCF procedure.[6]

Molecular geometries will be specified by the Jacobi coordinates $\mathbf{R} = (R,r,\gamma)$ where r is the H^1-H^2 distance, R is the distance between Al and the center of mass of H_2, and γ is the angle between the line segments corresponding to R and r, such that $\gamma = 90°$ for C_{2v} geometries. See Figure 1. Points, $\mathbf{R}_x$, on the seam of conical intersections will be parametrized by r, that is $\mathbf{R}_x(r) \equiv [R(r), r, \gamma(r)]$. It will emerge that as the result of the trifurcation of the seam of conical intersection, $\mathbf{R}_x(r)$ is not a single-valued function of r. It will therefore be convenient to also denote points of conical intersection by $\mathbf{R}_{xj}$, where j is a number, usually defined in Table 1. As a consequence of the trifurcation, we shall encounter the situation $\mathbf{R}_x(r) = \{\mathbf{R}_{xj_1}, \mathbf{R}_{xj_2}, \mathbf{R}_{xj_3}\}$.

A. AlH_2 Wave Functions. The calculations employ Al (10s7p3d) and H (6s3p1d) contracted Gaussian basis sets. The $\Psi_I(\mathbf{r};\mathbf{R})$ are described at the second-order CI level[8] based on a five-electron, six-orbital (5a′, 1a″) active space, comprising the Al(3s,3p) orbitals and the H(1s) orbitals and resulting in 264 775 CSFs.

B. Characterization of a Conical Intersection. In the vicinity of an $\mathbf{R}_x$ the wave functions, and hence the energies and derivative couplings, for the $1^2A'$ and $2^2A'$ states (denoted I and J) can be described in terms of a set of characteristic parameters,[5] $\mathbf{g}^{IJ}(\mathbf{R}_x)$, $\mathbf{h}^{IJ}(\mathbf{R}_x)$ and $\mathbf{s}^{IJ}(\mathbf{R}_x)$:

$$g^I{}_\tau(\mathbf{R}) = \mathbf{c}^I(\mathbf{R}_x)^\dagger \frac{\partial \boldsymbol{H}(\boldsymbol{R})}{\partial \tau}\mathbf{c}^I(\mathbf{R}_x) \tag{4a}$$

$$h^{IJ}{}_\tau(\mathbf{R}) = \mathbf{c}^I(\mathbf{R}_x)^\dagger \frac{\partial \boldsymbol{H}(\boldsymbol{R})}{\partial \tau}\mathbf{c}^J(\mathbf{R}_x) \tag{4b}$$

$$\mathbf{g}^{IJ}(\mathbf{R}) = \mathbf{g}^J(\mathbf{R}) - \mathbf{g}^I(\mathbf{R}) \tag{4c}$$

$$\mathbf{s}^{IJ}(\mathbf{R}) = [\mathbf{g}^I(\mathbf{R}) + \mathbf{g}^J(\mathbf{R})]/2 \tag{4d}$$

These parameters, which can be readily determined using analytic gradient techniques,[9] enable determination of the energies and the largest part of the derivative coupling in the vicinity of a conical intersection.[5] In the analysis it is convenient to replace the Jacobi coordinates with canonical coordinates, ρ, θ, z, defined as follows. In the $g-h(\mathbf{R}_x)$ plane, defined by the vectors $\mathbf{g}^{IJ}(\mathbf{R}_x)$ and $\mathbf{h}^{IJ}(\mathbf{R}_x)$, define polar coordinates ρ, θ by $x = \rho \cos\theta$, $y = \rho \sin\theta$, where $x[y]$ is the displacement along $\hat{\mathbf{x}} \equiv \hat{\mathbf{h}}^{IJ}(\mathbf{R}_x)[\hat{\mathbf{y}} \equiv \hat{\mathbf{g}}^{IJ}(\mathbf{R}_x)^\perp]$, a unit vector in nuclear coordinate space parallel [perpendicular] to $\mathbf{h}^{IJ}(\mathbf{R}_x)$. Also let z represent a displacement along the unique axis perpendicular to the $g-h(\mathbf{R}_x)$ plane.

To first order in displacements from $\mathbf{R}_x$, $E_I(\mathbf{R})$ and $E_J(\mathbf{R})$ [for $I = -$, $J = +$, and $\mathbf{R} = (\rho,\theta,z)$] are given by

$$E_\pm(\rho,\theta,z) \cong E^{\mathrm{p}}_\pm(\rho,\theta,z) \equiv \epsilon_\pm(\rho,\theta,) + H(\rho,\theta,z;\mathbf{s}) \equiv \epsilon_\pm(\rho,\theta) + s_x x + s_y y + s_z z \tag{5}$$

where

$$\epsilon_\pm(\rho,\theta) = \pm\rho q(\theta) \tag{6a}$$

$$q(\theta)^2 = h^2\cos^2\theta + (g_x\cos\theta + g_y\sin\theta)^2 \equiv h^2\cos^2\theta + g^2\sin^2(\theta+\alpha) \tag{6b}$$

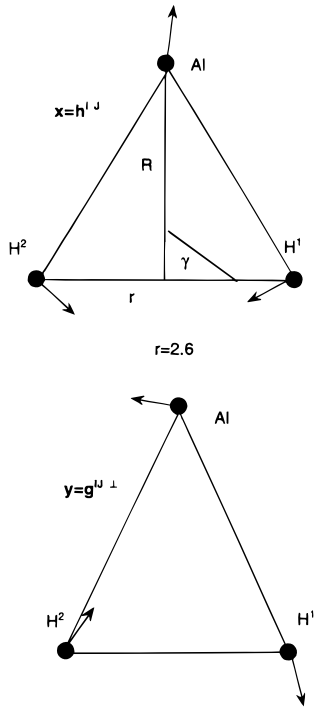

Figure 1. Unit vectors in the directions $\mathbf{h}^{IJ}(\mathbf{R}_x(2.6))$ and $\mathbf{g}^{IJ}(\mathbf{R}_x(2.6))^\perp$ [the component of $\mathbf{g}^{IJ}(\mathbf{R}_x(2.6))$ in the $g-h$ plane perpendicular to $\mathbf{h}^{IJ}(\mathbf{R}_x(2.6))$], represented in terms of atomic displacements. Also displayed are the Jacobi coordinates, R, r, γ.

TABLE 1: Points of Conical Intersection for AlH_2

	R (a_0)	r (a_0) γ (deg)	E (eV)	h (au)	**g** (au)[b]	**s** (au)[b]
			C_{2v}			
1	2.522	2.6 90.0	1.830	0.0523	0.0503 0.0155	−0.0364 −0.0050 −0.0965
2	2.647	2.8 90.0	1.492			
3	2.759	3.0 90.0	1.338			
4	2.954	3.4 90.0	1.323			
5	3.193	4.0 90.0	1.623			
6	3.335	4.4 90.0	1.910			
			C_s[c]			
7	2.812	3.1 89.3	1.307	0.0601	0.0261 0.0025	0.0193 0.0066 −0.0062
8	2.895	3.3 77.5	1.426	0.0076	−0.0173 0.0584	−0.0131 0.0155 −0.0238
9	2.859	3.4 58.7	2.651			
10	2.828	3.493 49.41	4.593			

[a] $E = E_{1^2A'} \approx E_{2^2A'}$ relative to $E_{1^2A'}[Al+H_2] = -243.096\,687\,23$ au. [b] Presented in the order x, y, z. [c] By symmetry these points occur in pairs for γ (denoted $\mathbf{R}_{xn}$) and $180° - \gamma$ (denoted $\mathbf{R}_{xn'}$).

and

$$g_w = (1/2)\mathbf{g}^{IJ}(\mathbf{R}_x)\cdot\hat{\mathbf{w}} \qquad w = x, y \tag{7a}$$

$$h = \mathbf{h}^{IJ}(\mathbf{R}_x)\cdot\hat{\mathbf{x}} \tag{7b}$$

$$s_w = \mathbf{s}^{IJ}(\mathbf{R}_x)\cdot\hat{\mathbf{w}} \qquad w = x, y, z \tag{7c}$$

Here and subsequently the superscript p indicates the use of

perturbation theory. It can also be shown that[5]

$$f_\theta^{JI}(\mathbf{R}) \cong f_\theta^{p,JI}(\mathbf{R}) \equiv (1/2)\frac{gh\sin(\alpha+\pi/2)}{q^2(\theta)} \qquad (8)$$

Below it will be convenient to denote as $C(O,\rho)$ circular paths in the $g-h$ plane with origin O and radius ρ. Also $w[C]$ will denote the set of values of a function $w(\mathbf{R})$ on C and *max*-$w[C]$ will denote the maximum of that set of values.

As noted in the Introduction, $\mathbf{R}_x$ cannot be a true transition state. This can be seen from eqs 5 and 6. From these equations we have that $E_I(\mathbf{R})$ is the sum of two "linear" terms: $H(\rho,\theta,z)$ (usually nonvanishing) and a strictly negative contribution $\rho q(\theta)$. Thus, for $O = \mathbf{R}_x$ and ρ small, $E_I[C(O,\rho)]$ cannot look as it would if O were a saddle point, in two dimensions. This point is discussed further in section III (Figure 5).

C. The Adiabatic Correction near a Conical Intersection. In addition to providing for interstate transitions the derivative coupling, $\mathbf{f}^{JI}(\mathbf{R})$, can effect the nuclear motion through the adiabatic correction.[10] The adiabatic correction is added to $E_I(\mathbf{R})$ to produce an effective potential for nuclear motion:[11]

$$\bar{E}_I(\mathbf{R}) = E_I(\mathbf{R}) + [\sum_{\alpha=1}(2M_\alpha)^{-1}\sum_{K=1}^{N^{CSF}}|\mathbf{f}_\alpha^{KI}(\mathbf{R})|^2] \qquad (9)$$

Here, $\mathbf{f}_\alpha^{JI}(\mathbf{R}) = (f_{X_\alpha}^{JI}(\mathbf{R}), f_{Y_\alpha}^{JI}(\mathbf{R}), f_{Z_\alpha}^{JI}(\mathbf{R}))$, and X_α, Y_α, Z_α are the Cartesian coordinates of the αth nucleus with mass M_α. $f_\theta^{JI}(\mathbf{R})$ is key since as $\rho \to 0$, $f_\tau^{JI}(\mathbf{R})$ for $\tau = \rho, z$ are uniformly small while $(1/\rho)f_\theta^{JI}(\mathbf{R})$ is singular. Thus the singular character of $(1/\rho)f_\theta^{JI}(\mathbf{R})$ causes the nuclear motion to avoid points of conical intersection.

III. Results and Discussion

Table 1 presents points on the $1^2A'-2^2A'$ seam of conical intersection. For $r < 3.1\ a_0$ the seam has exclusively C_{2v} symmetry. The form of the seam is discussed in detail below. From this table the MECP, $\mathbf{R}_{mex}$, is predicted (based on a three-point quadratic fit) to be $\mathbf{R}_{mex} = (2.87, 3.22, 90°)$ with $E_{1^2A'}(\mathbf{R}_{mex}) = E_{2^2A'}(\mathbf{R}_{mex}) = 1.29$ eV (measured relative to Al + H_2; see Table 1). $\mathbf{R}_{mex}$ represents the lowest point on the C_{2v} ridge separating Al(^{2}P) + H_2 from $AlH_2(X^2A_1)$ and gives the "barrier" height for the C_{2v} path from Al + H_2 to AlH_2-(X^2A_1) starting on the $^2B_2$ potential energy surface. This prediction for $\mathbf{R}_{mex}$ is in good accord with a previous determination using a larger atomic orbital basis set,[3] which gave $R = 2.853\ a_0$, $r = 3.175\ a_0$, $\gamma = 90°$(assumed), and $E_{1^2A'}(\mathbf{R}_{mex}) = E_{2^2A'}(\mathbf{R}_{mex}) = 1.17$ eV. To put these energetics in perspective in the context of channel 1b, note that the $AlH(X^1\Sigma^+)$ + H asymptote is computed (measured) to be endoergic relative to Al + H_2 by 1.53(1.59) eV and is therefore only 0.23 eV above $E_{1^2A'}(\mathbf{R}_{mex})$. The predicted reaction endoergicity is in excellent accord with the experimental value given parenthetically.[4]

A. The Seam of Conical Intersection for $r \leq 3.1\ a_0$. Consider the local topology of the C_{2v} ridge starting with $\mathbf{R}_{x1} \equiv \mathbf{R}_x(2.6) = (2.522, 2.6, 90°)$. Figure 1 depicts $\hat{\mathbf{g}}^{IJ}(2.6)^\perp \equiv \hat{\mathbf{g}}^{IJ}(\mathbf{R}_x(2.6))^\perp$ and $\hat{\mathbf{h}}^{IJ}(2.6) \equiv \hat{\mathbf{h}}^{IJ}(\mathbf{R}_x(2.6))$. These two directions are perpendicular to the ridge. From this figure it is seen that the x-axis describes principally R and r motion. Motion along the positive x-axis is in the direction of the reactant (Al + H_2) channel. The y-axis, along $\hat{\mathbf{g}}^{IJ}(2.6)^\perp$, is largely the C_{2v} breaking, γ or antisymmetric stretch, motion and leads to the AlH + H channel. The z-axis is tangent to the ridge (that is, tangent to the seam of conical intersection) and is comprised of the R, r motion orthogonal to $\hat{\mathbf{h}}^{IJ}(2.6)$. Note that although $\mathbf{R}_x(2.6)$ has C_{2v} symmetry, the vectors $\mathbf{g}^{IJ}(2.6)$ and $\mathbf{h}^{IJ}(2.6)$ do not fully reflect this symmetry. This illustrates the fact that at a point

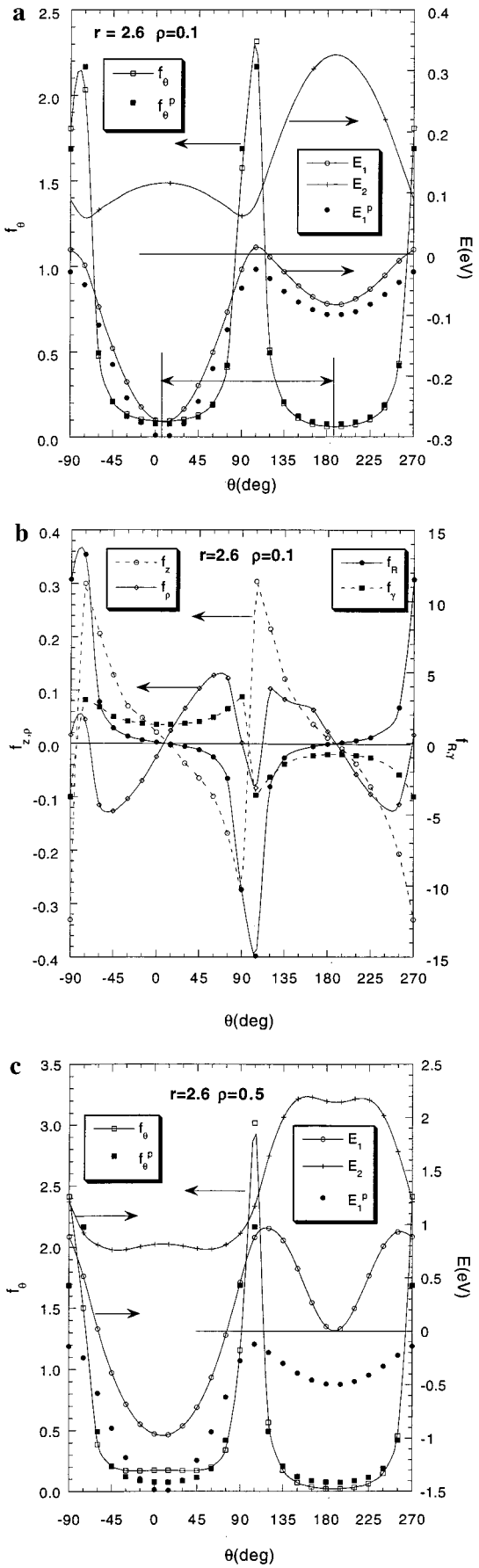

Figure 2. (a) For $\rho = 0.1$, $E_{1^2A'}[C(\mathbf{R}_x(2.6), \rho)]$ (open circles), $E_{2^2A'}[C(\mathbf{R}_x(2.6), \rho)]$ (pluses), and $f_\theta[C(\mathbf{R}_x(2.6), \rho)]$ (open squares), $E^p_{1^2A'}[C(\mathbf{R}_x(2.6), \rho)]$ (closed circles), and $f^p_\theta[C(\mathbf{R}_x(2.6), \rho)]$ (filled squares). Energies in eV relative to $E_{1^2A'}(\mathbf{R}_x(2.6)) = -243.029\ 438\ 6$ au. (b) $f_\tau[C(\mathbf{R}_x(2.6), 0.1)]$ $\tau = \rho$ (open diamonds), z (open circles), R(filled circles), γ (filled squares). (c) Same as part a with $\rho = 0.5$.

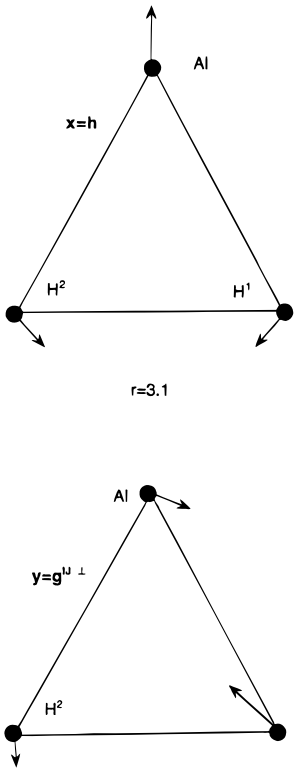

Figure 3. Unit vectors in the directions $\mathbf{h}^{IJ}(\mathbf{R}_x(3.1))$ and $\mathbf{g}^{IJ}(\mathbf{R}_x(3.1))^{\perp}$ represented in terms of atomic displacements.

of conical intersection $\mathbf{c}^I(\mathbf{R}_x)$ and $\mathbf{c}^J(\mathbf{R}_x)$ are only defined up to a one-parameter rotation.[5] Computationally, a small deviation from exact C_{2v} symmetry gives rise to eigenstates that are mixtures of $^2A_1$ and $^2B_2$ wave functions. However the $\hat{\mathbf{g}}^{IJ}(2.6)^{\perp}$ and $\hat{\mathbf{h}}^{IJ}(2.6)$ directions, in the uniquely determined $g-h(\mathbf{R}_x)$ plane, remain conceptually significant.

Figure 2a reports $E_I[C(\mathbf{R}_x(2.6), 0.1)]$, $I = 1,2^2A'$ and $f_\theta[C(\mathbf{R}_x(2.6), 0.1)]$ (the *IJ* superscript is suppressed here and below) and compares them with the perturbation theory results, $E^{\mathrm{p}}_{1^2A'}[C(\mathbf{R}_x(2.6), 0.1)]$ and $f^{\mathrm{p}}_\theta[C(\mathbf{R}_x(2.6), 0.1)]$ from eqs 5 and 8. Since $\mathbf{R}_x(2.6)$ has C_{2v} symmetry, half the data in this figure is symmetry redundant and the unique domain is indicated. The unique domain does not correspond exactly to $0° \le \theta \le 180°$ since the *y*-axis, for reasons explained above, does not correspond to the γ direction. If it had, s_y would be zero by symmetry. See Table 1.

For this small value of ρ, the perturbation theory results, $E^{\mathrm{p}}_{1^2A'}(\mathbf{R})$, $f^{\mathrm{p}}_\theta(\mathbf{R})$, which reflect exclusively the conical behavior, are expected, and are seen, to be in qualitatively good agreement with the MCSCF/CI results, $E_{1^2A'}(\mathbf{R})$, $f_\theta(\mathbf{R})$ although important and illuminating quantitative differences exist. Displacements along $\hat{\mathbf{h}}^{IJ}(2.6)$ ($\theta = 0°$, 180°) are significantly downhill in energy for both $E_{1^2A'}(\mathbf{R})$ and $E^{\mathrm{p}}_{1^2A'}(\mathbf{R})$; that is, the fall off from the ridge is steep. This may be verified by comparison with Figure 2c, which presents the $\rho = 0.5$ results. The asymmetry for positive and negative displacements along $\hat{\mathbf{h}}^{IJ}(2.6)$ ($\theta = 0°$, 180°) reflects the s_x contributions. For displacements along $\hat{\mathbf{g}}^{IJ}(2.6)^{\perp}$, ($\theta = -90°$, 90°), also perpendicular to the ridge, the energy changes less drastically; that is, in this direction the ridge is comparatively flat.

$E_{1^2A'}(\mathbf{R})$, for $\rho = 0.1$ and $\theta = -90°$ or 90°, are *greater* than $E_{1^2A'}(\mathbf{R}_x(2.6))$. Thus $E_{1^2A'}[C(\mathbf{R}_x(2.6), 0.1)]$, determined from the MCSCF/CI treatment, resembles the energetics on a loop surrounding a saddle point in *two* dimensions. However for the perturbation theory results for $E^{\mathrm{p}}_{1^2A'}(\mathbf{R})$, for $\rho = 0.1$ and $\theta = -90°$ or 90°, are *less* than $E_{1^2A'}(\mathbf{R}_x(2.6))$. This demonstrates that for smaller ρ $E_{1^2A'}[C(\mathbf{R}_x(2.6), \rho)]$ would not resemble the energetics of a two-dimensional saddle point; that is, as noted above, a conical intersection cannot be a true saddle point. The energetics in the third direction are discussed below.

Figure 2b reports $f_\tau[C(\mathbf{R}_x(2.6), 0.1)]$, for $\tau = \rho$, *z* and γ, *R*. In the canonical coordinate representation $f_\tau[C(\mathbf{R}_x(2.6), 0.1)]$, for $\tau = \rho$, *z*, is uniformly small, while $(1/\rho)f_\theta[C(\mathbf{R}_x(2.6), 0.1)]$, the *only* singular component as $\rho \to 0$, is strongly peaked at $\theta = -90°$, 90°. This peaking mirrors $\Delta E \equiv E_{2^2A'} - E_{1^2A'}$ as required by eqs 5 and 8, and can be viewed as a consequence of the asymmetry parameters, *g*/*h* and α. To see this, note that eq 8 can be rewritten as

$$f^{\mathrm{p},JI}_\theta(\rho,\theta) = (1/2)\frac{\sin(\alpha + \pi/2)}{(h/g)\cos^2\theta + (g/h)\sin^2(\theta + \alpha)} \quad (10)$$

For exact C_{2v} wave functions $\alpha = 0$. Then if $g/h = 1$, as in the case of C_{3v} symmetry,[12] $f^{\mathrm{p},JI}_\theta(\rho,\theta) = 1/2$ independent of ρ, θ, that is, no peaking.

In the Jacobi representation the situation is less intuitive. The three derivative couplings, $\tau = R$, *r*, and γ, are large, except as required by symmetry. See Figure 2b, where, for example, $f_\gamma(\rho,\sim 90°) \approx f_R(\rho,\sim 180°) = 0$. Recall that ΔE is minimized near $\theta = 90°$. Further, all three components are singular as $\rho \to 0$. Thus the Jacobi representation provides, in a sense, a misleading picture of the nature of the singularity at a conical intersection.

Figure 2c reports $E_I[C(\mathbf{R}_x(2.6), 0.5)]$, $I = 1,2^2A'$, and $f_\theta[C(\mathbf{R}_x(2.6), 0.5)]$ and, for comparison, $E^{\mathrm{p}}_{1^2A'}[C(\mathbf{R}_x(2.6), 0.5)]$, $f^{\mathrm{p}}_\theta[C(\mathbf{R}_x(2.6), 0.5)]$. For this larger ρ, $E_{1^2A'}$ is considerably different from $E^{\mathrm{p}}_{1^2A'}$. The peaking of $f_\theta(\rho,\theta)$ near $\theta = -90°$, 90°, evinced in the $\rho = 0.1$ results, remains evident in the $\rho = 0.5$ data, although in this case $E_{1^2A'}$ at $\theta = -90°$, 90° is much larger than $E_{1^2A'}(\mathbf{R}_x(2.6))$. Compare Figure 2, parts a and c. Also note that $max\text{-}E_{1^2A'}[C(\mathbf{R}_x(2.6), 0.5)]$ is much greater than $max\text{-}E_{1^2A'}[C(\mathbf{R}_x(2.6), 0.1)]$. As discussed by Mead[13] and subsequently by Kupperman,[14] when the total energy available to a system exceeds the energy along a closed loop surrounding a conical intersection, the geometric phase effect,[15−18,11] may alter the results of an adiabatic, that is, single potential energy surface, nuclear dynamics calculation. Here only small ρ loops will be relevant in this regard.

We next turn to the region of $\mathbf{R}_{x7} \equiv \mathbf{R}_x(3.1)$, which is near the MECP. The $g-h(r)$ planes, equivalently the tangents to the seam direction $\hat{\mathbf{z}}$, are approximately parallel for the range $r = 2.6-3.0$. This is not required by C_{2v} symmetry, which only guarantees that $\hat{\mathbf{z}}$ is orthogonal to the γ-direction. $\mathbf{R}_x(3.1)$ evinces a slight deviation from C_{2v} symmetry, which is also reflected in $\hat{\mathbf{z}}$. This symmetry breaking, which is reflected in $\hat{\mathbf{g}}^{IJ}(3.1)^{\perp}$ shown in Figure 3, is not an artifact of the calculation but a harbinger of the intersecting seams of conical intersections discussed in detail below. Note that $\hat{\mathbf{h}}^{IJ}(3.1) \approx +\hat{\mathbf{h}}^{IJ}(2.6)$, whereas $\hat{\mathbf{g}}^{IJ}(3.1)^{\perp} \approx -\hat{\mathbf{g}}^{IJ}(2.6)^{\perp}$. (Compare Figures 1 and 3).

The energetics and derivative couplings in the vicinity of $\mathbf{R}_x(3.1)$ and $\mathbf{R}_x(2.6)$ although qualitatively similar differ in important ways. This is demonstrated in Figure 4a, which reports $E_I[C(\mathbf{R}_x(3.1), 0.1)]$, $I = 1,2^2A'$, $f_\theta[C(\mathbf{R}_x(3.1), 0.1)]$ together with $E^{\mathrm{p}}_{1^2A'}[C(\mathbf{R}_x(3.1), 0.1)]$, $f^{\mathrm{p}}_\theta[C(\mathbf{R}_x(3.1), 0.1)]$, and in Figure 4b, which reports $f_\tau[C(\mathbf{R}_x(3.1), 0.1)]$, for $\tau = \rho$, *z*. Note the increased asymmetry between the $\theta \approx 270°$ and $\theta \approx 90°$ values of the energies and derivative couplings for $\mathbf{R}_x(3.1)$, when compared with $\mathbf{R}_x(2.6)$. The asymmetry would be absent if $\mathbf{R}_x(3.1)$ were a true C_{2v} structure. More significantly, although $f_\theta[C(\mathbf{R}_x(r), 0.1)]$ is peaked near $\theta = 270°$ (and 90°) for both *r* = 2.6 and 3.1, the peaking is much more extreme for $r = 3.1$ than $r = 2.6$. This could be anticipated from the characteristic parameters in Table 1. Thus nonadiabatic effects are expected

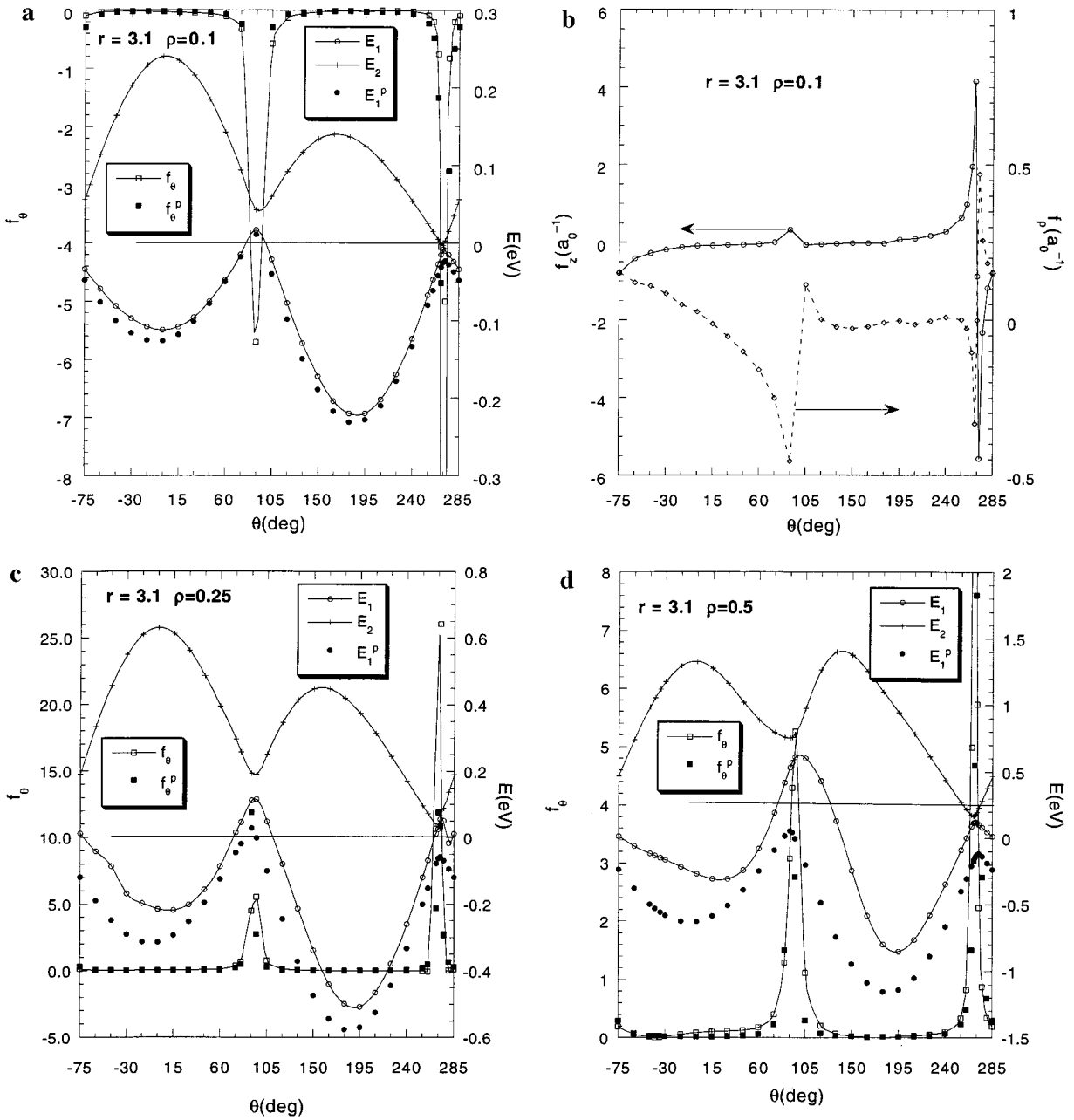

Figure 4. (a) For $\rho = 0.1$ $E_{1^2A'}[C(\mathbf{R}_x(3.1), \rho)]$ (open circles), $E_{2^2A'}[C(\mathbf{R}_x(3.1), \rho)]$ (pluses), and $f_\theta[C(\mathbf{R}_x(3.1), \rho)]$ (open squares), $E^p{}_{1^2A'}[C(\mathbf{R}_x(3.1), \rho)]$ (closed circles), and $f^p_\theta[C(\mathbf{R}_x(3.1), \rho)]$ (filled squares). Energies in eV relative to $E_{1^2A'}(\mathbf{R}_x(3.1)) = -243.048\,657$ au. (b) $f_\tau[C(\mathbf{R}_x(3.1), 0.1)]$, $\tau = \rho$ (open diamonds) and z (open circles). (c) Same as part a for $\rho = 0.25$. (d) Same as part a for $\rho = 0.50$.

to be more pronounced near $\theta = -90°, 90°$, which from Figure 3 correspond to displacements leading to AlH + H, than for $\theta = 0°$, 180°, r, R displacements connecting the reactants and the dihydride, channel 1a. The strongly peaked derivative coupling results from mixing of CSFs with, qualitatively, AlH_2 (X^2A_1) and $AlH(X^1\Sigma^+)$ + H character.

For $\mathbf{R}_x(3.1)$ $E_{1^2A'}(\rho = 0.1, \theta = 270°)$ is lower than $E_{1^2A'}(\mathbf{R}_x(3.1))$, in contrast to the situation at $\mathbf{R}_x(2.6)$ described above. The good agreement between $E_{1^2A'}[C(\mathbf{R}_x(3.1), 0.1)]$ and $E^p_{1^2A'}[C(\mathbf{R}_x(3.1), 0.1)]$ indicates that for $\rho < 0.1$ $E_{1^2A'}[C(\mathbf{R}_x(3.1), \rho)]$ can be obtained from eq 5. This observation will be used below to discuss the energetics in the vicinity of $\mathbf{R}_x(3.1)$.

Figure 4c,d reports $E_I[C(\mathbf{R}_x(3.1), \rho)]$, $I = 1,2^2A'$, $f_\theta[C(\mathbf{R}_x(3.1), \rho)]$ for $\rho = 0.25$ and 0.5, respectively. Note that $max\text{-}E_{1^2A'}[C(\mathbf{R}_x(r), 0.5)] - E_{1^2A'}(\mathbf{R}_x(r))$ is appreciably smaller for $r = 3.1$ than $r = 2.6$. Thus closed loops, that is, paths that exhibit the geometric phase effect, will be energetically accessible at larger distances from $\mathbf{R}_x(3.1)$ than was the case for $\mathbf{R}_x(2.6)$. Compare Figures 2c and 4d.

The points in Figure 4a ($\rho = 0.1$) and 4c ($\rho = 0.25$) corresponding to $\theta = 270°$ denoted $\mathbf{R}_a \equiv (2.8395, 3.1588, 87.5°)$ and $\mathbf{R}_c \equiv (2.885, 3.25, 83°)$ are of particular interest. For these points ΔE becomes quite small and the corresponding derivative couplings are very large. This suggests the existence of additional points of conical intersection, which would *not* have C_{2v} symmetry. This point is considered further below.

It was suggested in the Introduction that $\mathbf{R}_x(3.1)$, approximately the MECP, is near the saddle point for reaction 1a. This point is addressed in Figure 5, which reports the $250° < \theta < 285°$ portion of $E_{1^2A'}[C(\mathbf{R}_x, \rho)]$ for $\rho = 0.01$, 0.05, 0.1, and 0.25. The $\rho = 0.01$ and 0.05 results were obtained from eq 5, that is without resorting to ab initio calculations. From these data a saddle point is evident near $\theta = 270°$ and $\rho = 0.05$ a_0. The reaction coordinate is approximately along the x-axis (the direction parallel to $d\theta$ at $\theta = 270°$), which is the approximate C_{2v} mode in Figure 3, as expected. Since ρ is

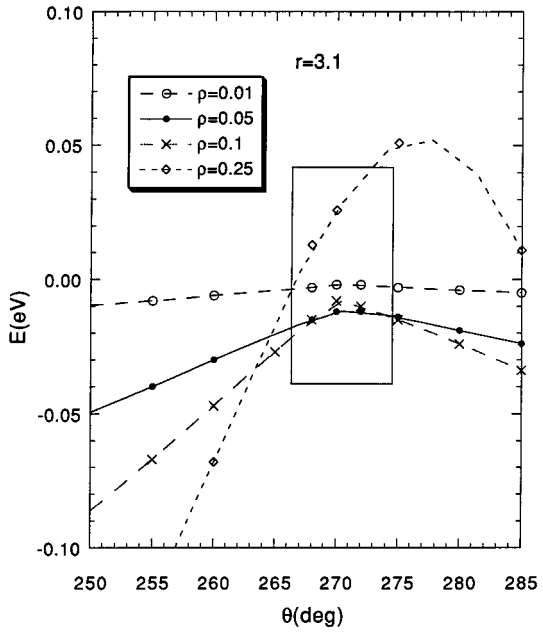

Figure 5. $E_{1^2A'}[C(\mathbf{R}_x(3.1), \rho)]$ for $\rho = 0.01, 0.05, 0.1, 0.25$, suggesting the existence of a saddle point near $\theta = 270°$. Energies in eV relative to $E_{1^2A'}(\mathbf{R}_x(3.1)) = -243.048\,657$ au.

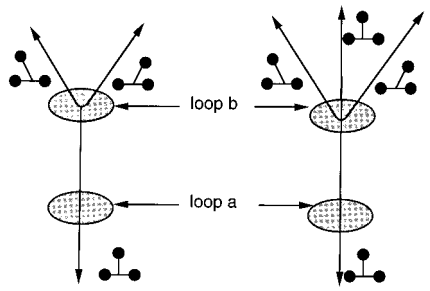

Figure 6. Closed loops around two seams of conical intersection. In the case of the trifurcation both loops a and b surround an odd number of conical intersections. For the bifurcation, loop a contains one conical intesection point while loop b contains two such points. Thus for the bifurcation the number of conical intersections enclosed by the closed loops can change suddenly from odd to even without encountering a singularity as one progresses from loop a to loop b. The arrows on the seam lines indicate that these lines do not terminate abruptly.

small, this region is quite close to the seam of conical intersections so nonadiabatic effects are expected to be preeminent. For this reason a more refined characterization of the transition state was not undertaken.

B. The seam of Conical Intersection for $r > 3.1\ a_0$. The preceding discussion indicates that the region of the seam of conical intersections near $\mathbf{R}_x(3.1)$ is quite complicated. As illustrated by the data in Figure 4, the $1,2^2A'$ surfaces remain quite close for a range of nuclear configurations. Since the C_s points of conical intersection in Table 1 occur in pairs (for $0° \le \gamma \le 180°$) denoted $\mathbf{R}_{xi}$ and $\mathbf{R}_{xi'}$, the data in that table indicate a trifurcation of the seam of conical intersection as r increases beyond 3.1 a_0. For example $\mathbf{R}_x(3.4) = \{\mathbf{R}_{x4}, \mathbf{R}_{x9}, \text{and } \mathbf{R}_{x9'}\}$. One branch continues for C_{2v} geometries while two symmetry equivalent branches exist with $\gamma \neq 90°$. See Figure 6. The points $\mathbf{R}_a = (2.8395, 3.1588, 87.5°)$ and $\mathbf{R}_c = (2.885, 3.25, 83°)$ suggested above to be near points of conical intersection are in fact quite close to the points $\mathbf{R}_{x7.25} = (2.836, 3.1588, 85.8°)$ and $\mathbf{R}_{x7.75} = (2.874, 3.25, 80.5°)$ obtained by linear interpolation from $\mathbf{R}_{x7}$ and $\mathbf{R}_{x8}$, Table 1. Similar trifurcations have been reported and analyzed in O_3[19] and CH_2.[20]

The occurrence of a trifurcation, two intersecting seams, rather than a bifurcation, in which the C_{2v} component of the seam disappears, has an important consequence illustrated in Figure 6. In the case of the trifurcation both loop a and loop b surround an odd number of conical intersection points (1 and 3, respectively) so that the geometric phase effect, more correctly the sign change in the electronic wave function, is obtained for such loops on either side of the trifurcation. For a bifurcation one would have the unappealing occurrence that the number of conical intersections enclosed by the closed loops could change suddenly from odd to even, as one progresses from loop a to loop b, so that the sign change in the electronic wave function would "disappear" abruptly, although the loops in question would never include a singular point.

C. Conical Intersections vs Narrowly Avoided Crossings. For $r \le 3.1\ a_0$ the (C_{2v}) seam of conical intersections was determined using C_s symmetry wave functions and an analytic gradient based algorithm discussed previously.[21] For $r > 3.1\ a_0$ the C_{2v} seam of conical intersection was found using equivalent wave functions with C_{2v} symmetry imposed. A numerical search algorithm can never rigorously distinquish between a point of conical intersection and a narrowly avoided crossing. One could determine whether in fact the points listed in Table 1 are points of conical intersections by considering the phase of the electronic wave functions for closed paths C surrounding the point in question, as was done by Ruedenberg in his seminal analysis of conical intersections in ozone.[22,23] However this can be quite tedious. Instead, here $X(C)$, the circulation of $\mathbf{f}^{IJ}$ for a small loop C around the point in question, will be used to consider this question. As a consequence of eq 8, it can be shown[5] that

$$X(C) = \oint_c \mathbf{f}^{IJ}(\mathbf{R})\cdot d\mathbf{R} = \int_0^{2\pi} f_\theta\, d\theta \xrightarrow[\rho\to 0]{} \kappa(C_\epsilon) \qquad (11)$$

where $\kappa(C_\epsilon) = 0$ if C_ϵ, the infinitesimal loop, contains 0 points of conical intersection and $\kappa(C_\epsilon) = \pi$ if C_ϵ contains 1 point of conical intersection. This approach has the advantage that the phase of the integrand at the end point of the loop is known, since $\mathbf{f}^{IJ}(\mathbf{R})$ does not change sign after traversing a closed loop. This provides a useful control in assigning of the phase of the integrand at neighboring points. The existence of three independent components for the derivative coupling vector $\mathbf{f}^{IJ}(\mathbf{R})$ can also help to decide phase relationships in otherwise ambiguous situations without the need to determine additional points.

$X(C)$ was determined for three representative loops $C_1 = (\mathbf{R}_{x8}, \rho = 0.2)$; $C_2 = (\mathbf{R}_{x5}, \rho = 0.1)$, and $C_3 = (\mathbf{R}_{x5} - 0.1_{\hat{\mathbf{y}}}, \rho = 0.05)$, where from Table 1 $\mathbf{R}_{x8} = (2.895, 3.3, 77.5°)$ and $\mathbf{R}_{x5} = (3.193, 4.0, 90°)$. C_1 and C_2 are suggested to contain a single point of conical intersection, whereas C_3 should contain no conical intersection points. The quadrature required to evaluate $X(C)$ was performed on the basis of spline interpolation of $f_\theta[C(O,\rho)]$, reported in Figure 7a for C_1 and Figure 7b for C_2 and C_3. We find $X(C_1) = (0.99687586)\pi$, $X(C_2) = (0.99190496)\pi$, and $X(C_3) = (-0.00000538)\pi$. $X(C_1)$ and $X(C_2)$ confirm that C_1 and C_2 in fact contain a point (actually an odd number of points) of conical intersection. $X(C_3)$ confirms that C_3 contains no (actually an even number of) conical intersections. The deviations of $X(C)$ from the $\rho = 0$ limit are expected since the derivative coupling is in general known to have a nonremovable part, a part with a nonvanishing curl.[24,25] Figure 7b illustrates the differences in $f_\theta[C(O,\rho)]$ that lead to $X(C_2) \approx \pi$ and $X(C_3) \approx 0$.

D. Implications for Nuclear Dynamics. As the saddle point for channel 1a lies near $\mathbf{R}_x(3.1)$, this region will play an important role in the dynamics of reaction 1. Excited vibrational levels of $AlH_2(X^2A_1)$, $AlH_2(X^2A_1, v^*)$, are resonances that are likely to sample this region of nuclear coordinate space during their decay. Thus a combination of experimental and theoretical

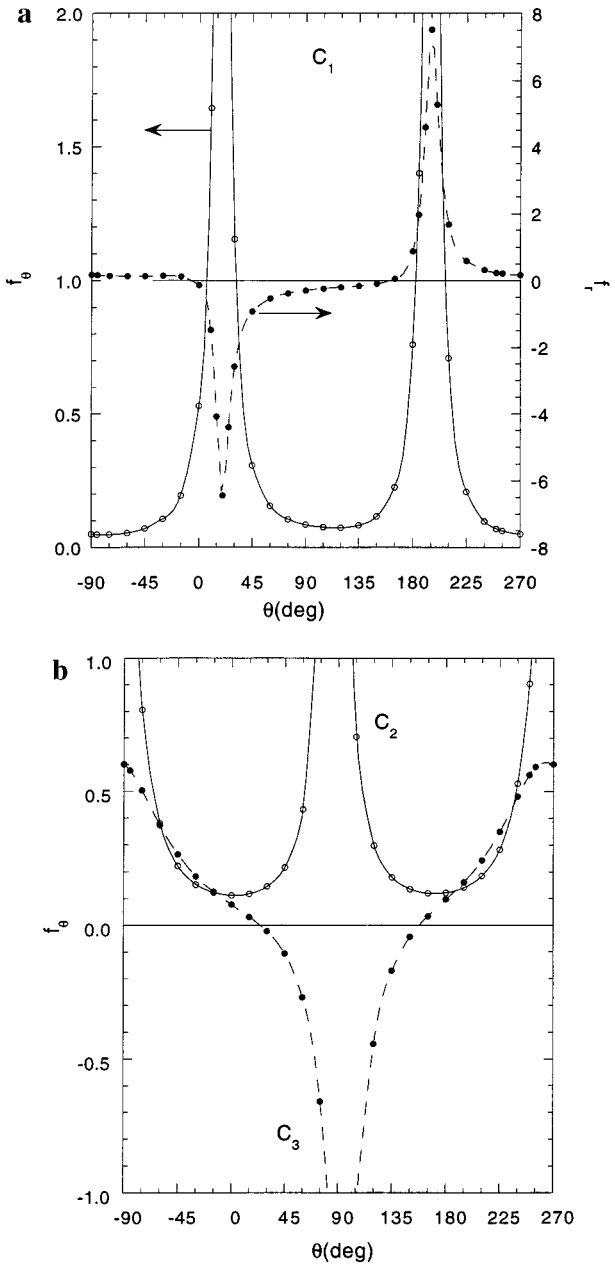

Figure 7. $f_\theta[C(O,\rho)]$: (a) $C_1 \equiv (\mathbf{R}_{x8}, \rho = 0.2)$; (b) C_2 ($\mathbf{R}_{x5}$, $\rho = 0.1$); and C ($\mathbf{R}_{x5}-0.1\hat{y}$, $\rho = 0.05$). In part a $f_r[C(O,\rho)]$ is also presented. $\mathbf{R}_{x8}$ = (2.895, 3.3,77.5°) and $\mathbf{R}_{x5}$ = (3.193, 4.0, 90°). Note that f_θ has a constant sign for C_1 and C_2, while f_θ changes sign for C_3. This accounts for the different values of $X(C)$ discussed in the text. The range of the ordinates is chosen to emphasize this point.

studies of the decay of these resonances would shed important light on the nonadiabatic dynamics. It will, for example, be interesting to see how the marked θ dependence of the derivative couplings evident in Figure 4a,b,d is reflected in the propensity for nonadiabatic dynamics in general and nonadiabatic recrossing in particular.

IV. Summary and Conclusions

The role of conical intersections in the ground-state reactions $Al(^2P)+H_2 \rightarrow AlH_2(X^2A_1)$ or $AlH(X^1\Sigma^+) + H$ has been considered. The energies and derivative couplings were computed in the vicinity of the seam of conical intersections. It was argued that wave packets describing the decomposition of $AlH_2(X^2A_1, \upsilon^*)$, excited vibrational levels of $AlH_2(X^2A_1)$, are likely to pass quite close to the minimum energy point on the seam of conical intersections. Nonadiabatic recrossing could serve to increase the observed lifetime of these resonances. Consequently the decay of these resonances provides a valuable laboratory for the study of nonadiabatic effects.

It will also be interesting to compare the conical intersections in AlH_2 with those in BH_2. The BH_2 van der Waals complex has been the object of previous theoretical[26,27] and experimental[28] studies. It has been suggested that the electronically excited $B(2s2p^2\ ^2D)-H_2$ van der Waals complex may decay radiationlessly to $BH(X^1\Sigma^+)$.[28]

The seam of conical intersections is shown to exhibit an unusual trifurcation. An exclusively C_{2v} region of the seam of conical intersection divides into a branch that preserves C_{2v} symmetry and two symmetry equivalent branches that have only C_s symmetry. Equivalently two seams of conical intersection, one with exclusively C_{2v} symmetry, intersect. The existence of conical intersections was demonstrated by analyzing the line integral of the derivative couplings along closed loops surrounding the point of conical intersection.

Acknowledgment. The calculations reported in this work were performed on D.R.Y.'s IBM RSC 6000 workstations purchased with funds provided by AFOSR Grant AFOSR 90-0051, NSF Grant CHE 91-03299, and DOE-BES Grant DE-FG02-91ER14189. D.R.Y. wishes to acknowledge illuminating conversations with Dr. B. Kendrick concerning *n*-furcations of a seam of conical intersection.

References and Notes

(1) Waschewsky, G. C. G.; Kash, P. W.; Myers, T. L.; Kitchen, D. C.; Butler, L. J. *J. Chem. Soc., Faraday Trans.* **1994**, *90*, 1581.
(2) Allison, T. C.; Mielke, S. L.; Schwenke, D. W.; Truhlar, D. G. *J. Chem. Soc., Faraday Trans.* **1997**, *93*, 825−832.
(3) Gordon, M. S.; Chaban, G.; Taketsugu, T. *J. Phys. Chem.* **1996**, *100*, 11512−11525.
(4) Huber, K. P.; Herzberg, G. *Molecular Spectra and Molecular Structure IV. Constants of Diatomic Molecules*; Van Nostrand Reinhold: New York, 1979.
(5) Yarkony, D. R. *J. Phys. Chem. A* **1997**, *101*, 4263−4270.
(6) Lengsfield, B. H.; Yarkony, D. R. In *State-Selected and State to State Ion−Molecule Reaction Dynamics: Part 2 Theory*; Baer, M., Ng, C.-Y., Eds.; John Wiley and Sons: New York, 1992; Vol. 82, pp 1−71.
(7) Shavitt, I. In *Modern Theoretical Chemistry*; Schaefer, H. F., Ed.; Plenum Press: New York, 1976; Vol. 3, p 189.
(8) Silverstone, H. J.; Sinanoglu, O. *J. Chem. Phys.* **1966**, *44*, 1899−1907.
(9) Yarkony, D. R. *J. Phys. Chem.* **1996**, *100*, 18612−18628.
(10) Jensen, J. O.; Yarkony, D. R. *J. Chem. Phys.* **1988**, *89*, 3853.
(11) Yarkony, D. R. *Rev. Mod. Phys.* **1996**, *68*, 985.
(12) Mead, C. A. *J. Chem. Phys.* **1983**, *78*, 807−814.
(13) Mead, C. A. *J. Chem. Phys.* **1980**, *72*, 3839.
(14) Kuppermann, A.; Wu, Y.-S. M. *Chem. Phys. Lett.* **1993**, *205*, 577.
(15) Longuet-Higgins, H. C. *Adv. Spectrosc.* **1961**, *2*, 429.
(16) Mead, C. A.; Truhlar, D. G. *J. Chem. Phys.* **1979**, *70*, 2284−2296.
(17) Berry, M. V. *Proc. R. Soc. London Ser. A* **1984**, *392*, 45−57.
(18) Mead, C. A. *Rev. Mod. Phys.* **1992**, *64*, 51−85.
(19) Atchity, G. J.; Ruedenberg, K.; Nanayakkara, A. *Theor. Chem. Acc.* **1997**, *96*, 195.
(20) Matsunaga, N.; Yarkony, D. R. *J. Chem. Phys.*, in press.
(21) Yarkony, D. R. In *Modern Electronic Structure Theory*; Yarkony, D. R., Ed.; World Scientific: Singapore, 1995; pp 642−721.
(22) Xantheas, S.; Elbert, S. T.; Ruedenberg, K. *J. Chem. Phys.* **1990**, *93*, 7519−7521.
(23) Xantheas, S. S.; Atchity, G. J.; Elbert, S. T.; Ruedenberg, K. *J. Chem. Phys.* **1991**, *94*, 8054−8069.
(24) Mead, C. A.; Truhlar, D. G. *J. Chem. Phys.* **1982**, *77*, 6090−6098.
(25) Yarkony, D. R. *J. Chem. Phys.* **1996**, *105*, 10456−10461.
(26) Alexander, M. *J. Chem. Phys.* **1993**, *99*, 6014.
(27) Alexander, M.; Yang, M. *J. Chem. Phys.* **1995**, *103*, 7956.
(28) Yang, X.; Hwang, E.; Dagdigian, P. J. *J. Chem. Phys.* **1996**, *104*, 8165.